



^{27}Al NMR studies of Ce–Al mixed oxides: origin of 40 ppm peak

R. Sasikala, V. Sudarsan, and S.K. Kulshreshtha*

Novel Materials and Structural Chemistry Division, Bhabha Atomic Research Centre, Trombay, Mumbai 400 085, India

Received 6 June 2002; received in revised form 12 August 2002; accepted 27 August 2002

Abstract

$\text{CeO}_2\text{-}\gamma\text{-Al}_2\text{O}_3$ mixed oxides have been prepared by using both co-precipitation and impregnation methods followed by calcination at 650°C and investigated by ^{27}Al MAS NMR, powder X-ray diffraction and temperature programmed reduction techniques to understand the nature of chemical interaction existing between CeO_2 and $\gamma\text{-Al}_2\text{O}_3$. The ^{27}Al NMR spectra of CeO_2 -containing samples showed an additional peak placed at 40 ppm along with the two peaks at 68 and 6 ppm which originate from the tetrahedrally and octahedrally coordinated Al^{3+} ions present in $\gamma\text{-Al}_2\text{O}_3$. As the concentration of CeO_2 in the mixed oxide increased, the intensity of the 40 ppm peak increased and this was the prominent peak for CeO_2 -rich mixed oxide samples. The origin of this 40 ppm peak is discussed and it is inferred that this peak is due to Al^{3+} ions, which are present in CeO_2 lattice, forming a solid solution.

© 2002 Elsevier Science (USA). All rights reserved.

Keywords: CeO_2 ; Al_2O_3 ; ^{27}Al NMR; 40 ppm peak; X-ray diffraction; TPR

1. Introduction

Ceria-promoted alumina is a well-known support material for automobile three-way catalysts [1–3]. Ceria exists in two different forms on alumina, namely as a dispersed phase and an aggregated phase. Based on a number of investigations, it has been reported that there exists a strong interaction between the dispersed ceria and alumina, but the nature of this interaction has not been well understood [4,5]. X-ray diffraction studies of $\text{CeO}_2\text{-}\gamma\text{-Al}_2\text{O}_3$ mixed oxides showed poor crystallinity for $\gamma\text{-Al}_2\text{O}_3$ phase and peaks mainly corresponding to CeO_2 were seen [4]. Based on X-ray absorption near-edge spectroscopy measurements, these authors also inferred that the dispersed phase of ceria contains Ce^{4+} with decreased ligand field effect due to relaxed coordination distances as compared to aggregated ceria and hence its reduction is facilitated. From XPS and Raman studies [5] of this system, it has been proposed that a precursor responsible for the formation of CeAlO_3 , exists in the dispersed phase and it has been suggested that this phase has Ce^{4+} stabilized in the

calcination vacancies on the surface of $\gamma\text{-Al}_2\text{O}_3$. Based on ^{27}Al NMR studies of such samples the coordination behavior of Al^{3+} in $\text{CeO}_2\text{-}\gamma\text{-Al}_2\text{O}_3$ has been investigated by Engler et al. [6]. For $\gamma\text{-Al}_2\text{O}_3$, these authors reported two distinct peaks characterized by chemical shift values of $\delta \sim 65$ and 5 ppm corresponding to the tetrahedral and octahedral sites of Al^{3+} present in this structure. On calcination at 1000°C and above, only one peak characterized by $\delta \sim 9$ ppm, corresponding to Al^{3+} in octahedral coordination is seen due to the transformation of $\gamma\text{-Al}_2\text{O}_3$ to $\alpha\text{-Al}_2\text{O}_3$. For $\text{CeO}_2\text{-}\gamma\text{-Al}_2\text{O}_3$ samples, these authors reported an additional peak at 36 ppm, which was thought to arise due to the interaction of Ce^{3+} with alumina. Vazquez et al. [7], have also reported a similar peak placed at ~ 35 ppm in the NMR spectra of lanthanum- and cerium-doped alumina samples which was assigned to the formation of a new compound due to the interaction of alumina with cerium/lanthanum wherein Al^{3+} ions are placed at the tetrahedral sites.

In order to have a better understanding of the origin of this peak seen in the region of 30–40 ppm in the ^{27}Al NMR spectrum of $\text{CeO}_2\text{-Al}_2\text{O}_3$ mixed oxides, a number of mixed oxide samples of $(\text{Al}_2\text{O}_3)_{1-x}(\text{CeO}_2)_x$ with $0.0 \leq x \leq 1.0$, have been prepared either by co-precipitation or impregnation methods and studied by powder

*Corresponding author. Fax: +91-22-5505151.
E-mail address: kulshres@magnum.barc.ernet.in
(S.K. Kulshreshtha).

X-ray diffraction and ^{27}Al MAS NMR techniques. Further, to confirm the role of Ce^{3+} in giving rise to the peak at ~ 36 ppm in these mixed oxides, as proposed by Engler et al., the temperature programmed reduction (TPR) studies of few representative mixed oxides were carried out in hydrogen atmosphere to produce Ce^{3+} and ^{27}Al NMR spectra of these reduced samples were recorded.

2. Experimental

Mixed oxides of Ce and Al with general formula $(\text{Al}_2\text{O}_3)_{1-x}(\text{CeO}_2)_x$ where $x = 0.10, 0.50, 0.80, 0.90$ and 0.95 , which will be referred to as C10A, C50A, C80A, C90A and C95A, respectively, were prepared by co-precipitation method from their respective nitrate solutions using NH_4OH as the precipitating agent. The precipitate was dried in an oven at $\approx 175^\circ\text{C}$ for nearly 18 h followed by heating in air at 650°C for 2 h. Samples of CeO_2 and Al_2O_3 , which were used as the oxide precursors for the preparation of impregnated samples using wet impregnation method, were also prepared by the same method. Impregnated sample of chemical composition $(\text{Al}_2\text{O}_3)_{0.9}(\text{CeO}_2)_{0.1}$ was prepared by impregnating the above-mentioned Al_2O_3 with cerium nitrate solution and hereafter referred as C10A-I. Similarly, another impregnated sample with chemical composition $(\text{Al}_2\text{O}_3)_{0.05}(\text{CeO}_2)_{0.95}$ was prepared by using the above-mentioned CeO_2 and aluminum nitrate solution and is hereafter referred as C95A-I. These samples were dried in an oven at $\approx 175^\circ\text{C}$ for nearly 18 h and afterwards heated at 650°C for 2 h in air so that the nitrates were fully decomposed to form corresponding oxides.

TPR studies were carried out from room temperature to 950°C in a quartz reactor with a heating rate of $15^\circ/\text{min}$ in $\text{H}_2 + \text{Ar}$ stream ($\sim 8\%$ H_2 by volume, flow rate = 32 ml/min). All samples were given an in situ pretreatment of heating in Ar flow at 650°C for 2 h followed by cooling to room temperature before TPR experiments. Change in concentration of H_2 in the effluent gas, due to the reduction of Ce^{4+} in these samples, was monitored by a thermal conductivity detector. The signal depicted in TPR curves is indicative of the volume of hydrogen consumed during this reduction process.

^{27}Al MAS NMR spectra were recorded with Bruker Avance DPX 300 machine with a basic frequency of 78.2034 MHz . The samples were packed in 7 mm diameter zirconia rotors and subjected to a spinning speed of up to 5000 Hz . Typical 90° pulse duration for MAS experiments was $4.5 \mu\text{s}$ with a relaxation delay of 4 s. Depending on the concentration of Al^{3+} in these samples, NMR spectra were recorded for different durations so as to get a reasonable signal to noise ratio.

Chemical shift values are reported with respect to $[\text{Al}(\text{H}_2\text{O})_6]^{3+}$ solution as standard. The position of isotropic peaks, for all samples, was identified by spinning them at different rates. Powder X-ray diffraction patterns were recorded by using Philips PW1820-X-ray diffractometer coupled with a PW 1729 generator, which was operated at 30 kV and 20 mA . Monochromatic $\text{CuK}\alpha$ radiation (wave length 1.54178 \AA), obtained by using a graphite crystal, was used for recording the X-ray diffraction patterns.

3. Results and discussion

XRD patterns of mixed oxide samples are shown in Fig. 1 along with those of CeO_2 and Al_2O_3 prepared in the same manner. It can be seen that the samples with $x \geq 0.5$, showed diffraction peaks characteristic of CeO_2 alone and as the Al content increased, CeO_2 exhibited poor crystallinity. Only C10A sample showed diffraction peaks corresponding to both CeO_2 and $\gamma\text{-Al}_2\text{O}_3$ phases with significantly lower intensity for $\gamma\text{-Al}_2\text{O}_3$. This observation is in conformity with the results reported by Martinez-Arias et al. [4] and is arising due to the poor crystallinity of $\gamma\text{-Al}_2\text{O}_3$ and the smaller value of X-ray scattering factor of Al in comparison to that of Ce. The addition of varying amounts of Al_2O_3 did not affect the unit cell parameters of CeO_2 phase implying that Al_2O_3 and CeO_2 do not form a bulk solid solution. XRD patterns of impregnated samples are found to be essentially similar to that of co-precipitated samples having the same chemical compositions.

Fig. 2 shows the ^{27}Al MAS NMR spectra of mixed oxide samples heated at 650°C along with that of $\gamma\text{-Al}_2\text{O}_3$. The NMR spectrum of $\gamma\text{-Al}_2\text{O}_3$ (Fig. 2(a)) shows two peaks placed at 68.2 and 6.6 ppm , which are assigned to tetrahedrally (Al_{tet}) and octahedrally (Al_{oct}) coordinated Al^{3+} . In $\text{CeO}_2\text{-Al}_2\text{O}_3$ mixed oxides (Fig. 2(b)–(h)), in addition to these peaks, a sharp peak at $\approx 40 \text{ ppm}$, growing in intensity with increase in CeO_2 concentration, is seen. As CeO_2 concentration increases, the relative intensity of Al_{oct} and Al_{tet} decreases systematically and ultimately for C95A only the 40 ppm peak is seen. This indicates that a different species containing Al^{3+} is present in these mixed oxides. From the comparison of the NMR spectra of samples prepared by co-precipitation and impregnation methods (viz. Fig. 2(b), (c), (g) and (h)), it is observed that they are qualitatively similar but with slight difference in their relative intensities.

For oxide samples, the ^{27}Al NMR peak observed in the region of $30\text{--}40 \text{ ppm}$, has been assigned to different types of Al^{3+} species and there exists disagreement in its assignment. For example, Wang et al. [8] reported a peak at 33.1 ppm in the ^{27}Al NMR spectra of nano-

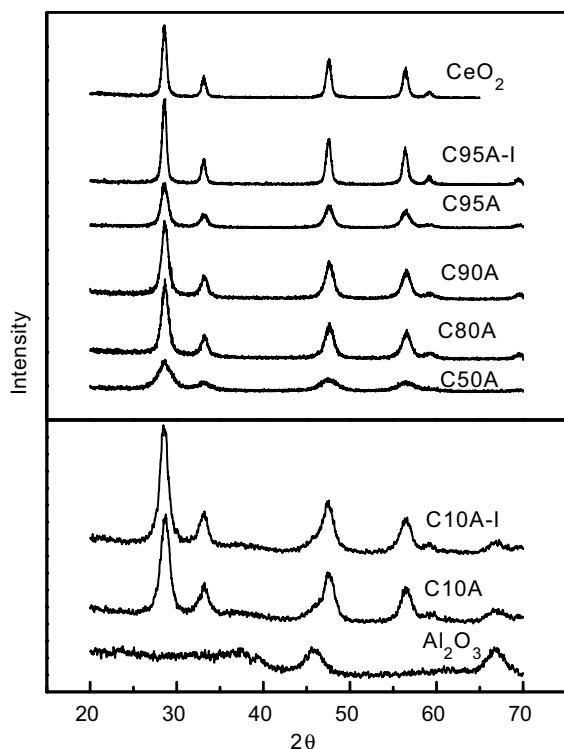


Fig. 1. XRD patterns of Ce–Al mixed oxides heated in air at 650°C for 2 h.

crystalline γ -alumina, which was assigned to Al^{3+} in an octahedral site with some of the lattice oxygen ions being substituted by hydroxyl groups [8]. In another study, involving a number of mixed oxides of Al_2O_3 with TiO_2 , SiO_2 and ZrO_2 , Miller and Lakshmi [9] observed a peak at ≈ 30 ppm besides peaks corresponding to octahedrally and tetrahedrally coordinated Al^{3+} . This peak was assigned to a penta-coordinated Al^{3+} and the line width of this peak was comparable to that of the octahedrally and tetrahedrally coordinated Al^{3+} . Mackenzie et al. [10] have some difference of opinion regarding the assignment of this peak to a penta-coordinated Al^{3+} . These authors have also reported a similar peak at ~ 30 ppm for the gel-driven mullite precursor, which was assigned to Al^{3+} species, having distorted tetrahedral environment in the region of an O-deficient tri-cluster, which constitutes a distinctive element of the mullite structure on recrystallization. However, the peak observed at ~ 40 ppm in our study is distinctly different from the peak reported at ~ 30 ppm in the earlier studies, as the line widths of these two peaks are significantly different.

In the following section, the applicability of the above-mentioned proposals will be examined to understand the origin of 40 ppm peak observed for CeO_2 - γ - Al_2O_3 mixed oxides. The 40 ppm peak, observed in our study, cannot be assigned to penta-coordinated Al^{3+} or replacement of some of oxygen ions by OH ions for

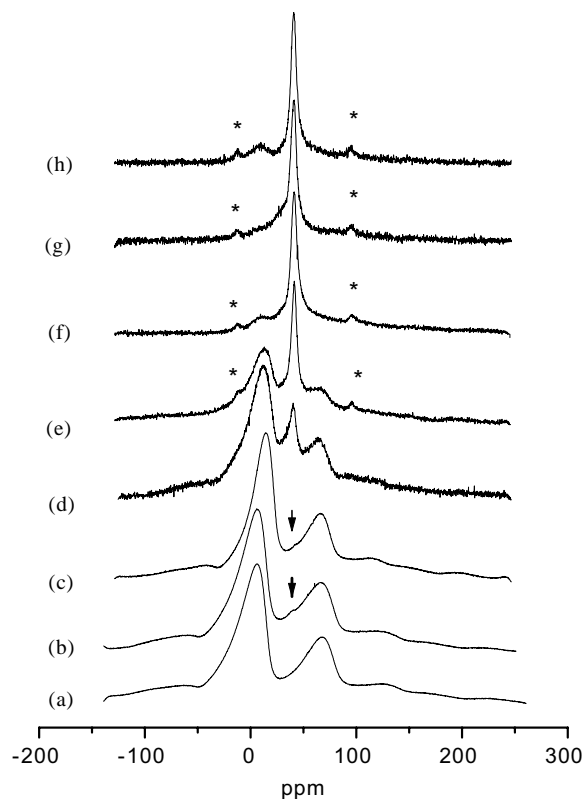


Fig. 2. NMR spectra of Ce–Al mixed oxides heated in air at 650°C for 2 h: (a) Al_2O_3 , (b) C10A, (c) C10A-I, (d) C50A, (e) C80A, (f) C90A, (g) C95A, and (h) C95A-I. The peak at 40 ppm is marked for C10A and C10A-I as it is very small. The peaks marked with asterisks correspond to spinning side bands.

octahedrally coordinated Al^{3+} , as the same is not seen for γ - Al_2O_3 , prepared by the same method used for CeO_2 - γ - Al_2O_3 mixed oxides. Further, a penta-coordinated Al^{3+} will give rise to at least comparable or more line width as compared to that of tetrahedrally or octahedrally coordinated Al^{3+} , due to the existence of residual second-order quadrupolar interactions due to its non-cubic site symmetry. This is unlike what has been observed for the 40 ppm peak, which has significantly lower line width as compared to the other peaks originating from the tetrahedral and octahedral coordination (viz. Fig. 2). In addition, this peak cannot be associated with the interaction of Ce^{3+} with Al^{3+} , as proposed by Engler et al. [6], because our method of preparation cannot give rise to Ce^{3+} ions in the original unreduced samples. This aspect is further discussed below in the light of the NMR results obtained for these samples after their TPR studies carried out in hydrogen stream.

TPR patterns of two representative samples namely, C95A and C90A, which both showed the dominant peak at 40 ppm in their ^{27}Al NMR patterns, are shown in Fig. 3 along with that of CeO_2 . The TPR pattern of CeO_2 shows two prominent peaks placed at $\sim 525^\circ\text{C}$ and 875°C arising due to surface and bulk reduction of

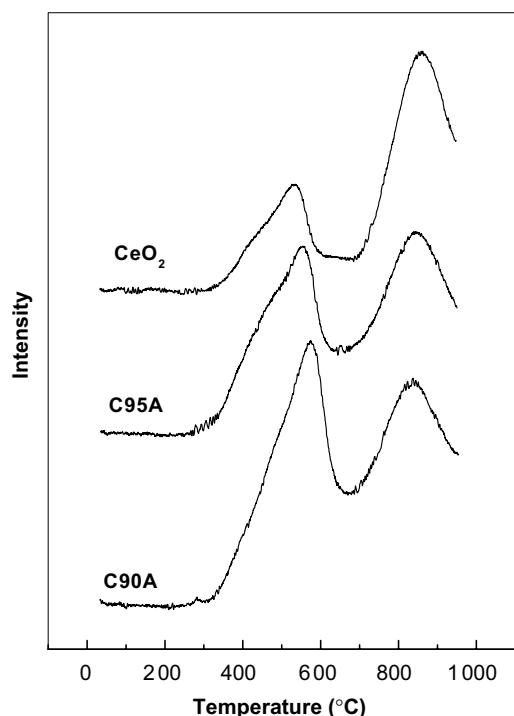


Fig. 3. TPR patterns of CeO_2 and Ce–Al mixed oxides.

CeO_2 . These results are quite similar to those reported by Yao and Yao [3] as well as by Fornasiero et al. [11] who have assigned these peaks to the reduction of Ce^{4+} to Ce^{3+} state. It can be seen that the TPR patterns of C95A and C90A are qualitatively similar to that of CeO_2 except that the relative intensity of these two peaks has increased slightly due to the increased surface area of Al^{3+} -containing samples as inferred from the increased width of the XRD peaks of these samples. From the volume of hydrogen consumed during TPR experiment of these samples, it is inferred that the reduction of CeO_2 is only partial and the average composition is close to $\text{CeO}_{1.85}$ for pure CeO_2 after TPR. Based on XPS study of $\text{CeO}_2/\text{Al}_2\text{O}_3$ sample containing 17% CeO_2 , the formation of Ce^{3+} has been established for the sample reduced under hydrogen stream at different temperatures up to 920°C and the formation of CeAlO_3 was suggested for this sample [5]. Fig 4(a) and (b) shows the ^{27}Al NMR spectra of C95A and C90A after their TPR experiments carried out upto 950°C . From the comparison of these spectra with those shown in Fig. 2(f) and (g) which correspond to the original samples, it can be seen that after TPR experiments, the intensity of 40 ppm peak has decreased significantly and an intense broad peak placed at ~ 0 ppm has appeared along with a very weak signal at 25 ppm. The intensity of 0 ppm peak is significantly more than that of 25 ppm peak. This implies that the peak at 40 ppm does not arise from the interaction of Ce^{3+} with Al^{3+} as suggested by Engler et al. [6]. The

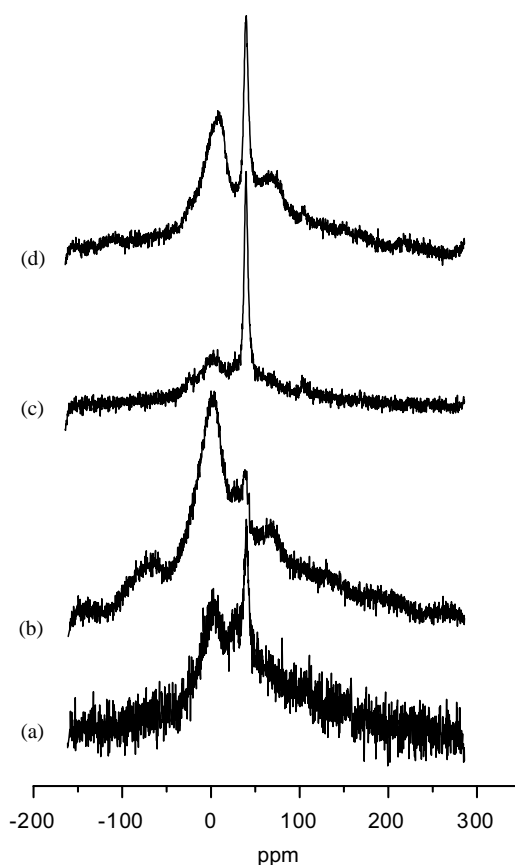


Fig. 4. NMR spectra of Ce–Al samples after TPR and reoxidation: (a) C95A, (b) C90A after TPR, (c) C95A and (d) C90A after their reoxidation at 850°C .

peak at ≈ 0 ppm is assigned to CeAlO_3 as inferred from the systematic evolution of this peak and the appearance of X-ray diffraction peaks characteristic of CeAlO_3 for samples having higher concentration of Al_2O_3 after their TPR experiments and their dependence on Al^{3+} concentration. The lower intensity peak observed at 25 ppm, is attributed to Al^{3+} , which have got Ce^{3+} in its vicinity produced by the partial reduction of Ce^{4+} . The paramagnetic nature of Ce^{3+} ions gives rise to an excess line width for both these peaks. Heating of these samples in oxygen at 850°C for 1 h resulted in NMR spectra which showed an intense peak at 40 ppm along with a pattern due to $\gamma\text{-Al}_2\text{O}_3$ which has segregated out in these samples, as can be seen from Fig. 4(c) and (d), respectively. The intense signal observed at 40 ppm for the oxidized samples indicates that Ce^{3+} , produced during TPR experiments, get oxidized to Ce^{4+} state during heating at 850°C in oxygen.

The other suggestion [5] that the distorted tetrahedral configuration produced by the presence of Ce^{4+} at the cation vacancies existing at the octahedral sites of $\gamma\text{-Al}_2\text{O}_3$, is also not applicable for this system. If that was the case, one should have observed the usual NMR signal due to Al^{3+} ions present at the octahedral sites as

it is not expected to be affected by the presence of Ce^{4+} at octahedral site. This is due to the fact that for $\gamma\text{-Al}_2\text{O}_3$ each octahedral Al^{3+} is surrounded by six tetrahedrally coordinated Al^{3+} ions as nearest-neighbour cations and each Al^{3+} at tetrahedral sites is surrounded by 12 Al^{3+} cations present at the octahedral sites. In such a situation, the presence of Ce^{4+} at the octahedral sites will affect the chemical shift of limited number of Al^{3+} cations present at the tetrahedral sites, as the number of Al^{3+} ions present at the octahedral sites is more than that of Ce^{4+} , which are occupying the vacant octahedral sites and the observed NMR spectrum should consist of usual signals due to both tetrahedral and octahedral Al^{3+} ions along with the additional signal originating due to the modified tetrahedral coordination of Al^{3+} caused by the presence of Ce^{4+} at octahedral sites. Further, the NMR signal for octahedrally coordinated Al^{3+} ions should always be stronger than the signal observed at 40 ppm as the number of Al^{3+} ions at octahedral sites is supposed to be ~ 1.66 times the number of Al^{3+} ions present at the tetrahedral sites in $\gamma\text{-Al}_2\text{O}_3$ structure. This is unlike the observed NMR spectrum of C95A (viz. Fig. 2(g)) where there is no clear signal due to the usual tetrahedral and octahedral Al^{3+} ions. Similarly, the NMR spectrum of the C95A-I sample, shown in Fig. 2(h), shows very poor signal due to Al^{3+} present at the tetrahedral and octahedral sites in comparison to the 40 ppm signal. Further, the smaller value of the ionic radius of Al^{3+} ($r_{\text{Al}^{3+}} = 0.051$ nm) as compared to Ce^{4+} ($r_{\text{Ce}^{4+}} = 0.103$ nm), facilitates the diffusion of Al^{3+} in the CeO_2 lattice and the diffusion of Ce^{4+} in $\gamma\text{-Al}_2\text{O}_3$ is expected to be difficult. This further rules out the possibility of the presence of Ce^{4+} at the octahedral sites in $\gamma\text{-Al}_2\text{O}_3$.

The most probable explanation for the appearance of 40 ppm peak in the NMR spectra of $\text{CeO}_2\text{-}\gamma\text{-Al}_2\text{O}_3$ mixed oxides, is the limited solubility of Al^{3+} ions in CeO_2 lattice. The formation of bulk solid solution between CeO_2 and $\gamma\text{-Al}_2\text{O}_3$ is prohibited because of significant difference in the ionic radii of Ce^{4+} and Al^{3+} ions and the difference in the crystal structure of CeO_2 and $\gamma\text{-Al}_2\text{O}_3$. The limited solubility of Al^{3+} in CeO_2 does not affect the unit cell parameters of CeO_2 to a measurable extent. The Al^{3+} ions located at Ce^{4+} sites in CeO_2 , possess cubic site symmetry with an eight-fold

coordination. The $\text{Al}^{3+}\text{-O}^{2-}$ bond distance for these Al^{3+} ions is mainly controlled by the CeO_2 crystal structure and affects their chemical shift value. Since these Al^{3+} ions do not experience any quadrupole interaction, they are expected to show a sharp NMR signal as has been observed in the present study for these $\text{CeO}_2\text{-Al}_2\text{O}_3$ mixed oxides. Another reason for observing a narrow line for these Al^{3+} , is the presence of Ce^{4+} cations as their nearest-neighbour cations which are diamagnetic in nature with nuclear spin $I = 0$ and do not contribute to any dipolar broadening to the NMR signal of these Al^{3+} ions.

4. Conclusion

^{27}Al MAS NMR studies of $\text{CeO}_2\text{-}\gamma\text{-Al}_2\text{O}_3$ mixed oxides have been carried out and an additional peak placed at ≈ 40 ppm along with the signals due to tetrahedrally and octahedrally coordinated Al^{3+} ions has been observed. This peak has been assigned to Al^{3+} ions, which are dissolved in CeO_2 lattice.

References

- [1] A. Piras, A. Trovarelli, G. Dolcetti, Appl. Catal. 28 (2000) L77–L81.
- [2] H. Ding, D. Weng, X. Wu, J. Alloys Compounds 311 (2000) 26–29.
- [3] H.C. Yao, Y.F.Y. Yao, J. Catal. 86 (1984) 254–265.
- [4] A. Martinez-Arias, M. Fernandez-Garcia, L.N. Salamanca, R.X. Valenzuela, J.C. Coneza, J. Soria, J. Phys. Chem. B 104 (2000) 4038–4046.
- [5] J.Z. Shyu, W.H. Weber, H.S. Gandhi, J. Phys. Chem. 92 (1988) 4964–4970.
- [6] B. Engler, E. Koberstein, P. Schubert, Appl. Catal. 48 (1989) 71–92.
- [7] A. Vasquez, T. Lopez, R. Gomez, B.A. Morales, O. Novaro, J. Solid State Chem. 128 (1997) 161–168.
- [8] J.A. Wang, X. Bokhimi, A. Morales, O. Novaro, T. Lopez, R. Gomez, J. Phys. Chem. 13 (1999) 299–303.
- [9] J.M. Miller, L.J. Lakshmi, J. Phys. Chem. B 102 (1998) 6465–6470.
- [10] K.J.D. MacKenzie, J.E. Meinhold, J.E. Patterson, M. Schneider, M. Somucker, D. Voll, J. Eur. Ceram. Soc. 16 (1996) 1299–1308.
- [11] P. Fornasiero, G. Balducci, R.D. Monte, J. Kaspar, V. Sergo, G. Gubitosa, A. Ferrero, M. Graziani, J. Catal. 164 (1996) 173–183.